University of Baghdad
College of Engineering
JOURNAL OF ENGINEERING

Journal of Engineering
journal homepage: www.joe.uobaghdad.edu.iq
Number 9 Volume 26 September 2020

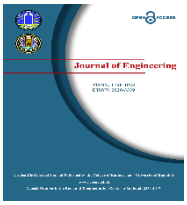

Mechanical and Energy Engineering

Buckling Behavior of Aluminum Alloy Thin-Walled Beam with Holes under Compression Loading

Dalya Salah Khazaal *
MSc student
Mechanical Engineering Dept.
University of Technology
me.19.18@grad.uotechnology.edu.iq

Hussein M. H. AL-Khafaji
Assistant Professor
Mechanical Engineering Dept.
University of Technology
hussalkhafaji@hotmail.com

Imad Abdulhussein Abdulsahib
Lecturer
Mechanical Engineering Dept.
University of Technology
20018@uotechnology.edu.iq

ABSTRACT

Thin-walled members are increasingly used in structural applications, especially in light structures like in constructions and aircraft structures because of their high strength-to-weight ratio. Perforations are often made on these structures for reducing weight and to facilitate the services and maintenance works like in aircraft wing ribs. This type of structures suffers from buckling phenomena due to its dimensions, and this suffering increases with the presence of holes in it. This study investigated experimentally and numerically the buckling behavior of aluminum alloy 6061-O thin-walled lipped channel beam with specific holes subjected to compression load. A nonlinear finite elements analysis was used to obtain the buckling loads of the beams. Experimental tests were done to validate the finite element results. Three factors namely; shape of holes, opening ratio D/D_O and the spacing ratio S/D_O were chosen to study their effects on the buckling strength of the channel beams. Finite elements results were obtained by using Taguchi method to identify the best combination of the three parameters for optimum critical buckling load, whereas determining the contribution of each parameter on buckling strength was implemented by using the analysis of variance technique (ANOVA) method. Results showed that the combination of parameters that gives the best buckling strength is the hexagonal hole shape, D/D_O=1.7 and S/D_O = 1.3 and the opening ratio (or size of holes) is the most effective on buckling behavior.
Keywords: thin-walled structure, buckling, nonlinear finite elements, holes, Taguchi method.

*Corresponding author
Peer review under the responsibility of University of Baghdad.
https://doi.org/10.31026/j.eng.2020.09.15

Article received: 4/5/2020
Article accepted:14/7/2020
Article published:1/9/2020

دراسة سلوك الانبعاج لعتبة رقيقة الجدران مصنوعة من سبيكة الالمنيوم بوجود ثقوب معرضة لحمل الانضغاط

داليا صلاح خزعل *
طالب ماجستير
قسم الهندسة الميكانيكية
الجامعة التكنولوجية/ بغداد

حسين محمد حسين الخفاجي
استاذ مساعد
قسم الهندسة الميكانيكية
الجامعة التكنولوجية/ بغداد

عماد عبد الحسين عبد الصاحب
مدرس
قسم الهندسة الميكانيكية
الجامعة التكنولوجية/ بغداد

الخلاصة

يتم استخدام الأعضاء ذوي الجدران الرقيقة بشكل متزايد في التطبيقات الهيكلية ، خاصة في الهياكل خفيفة الوزن كالانشاءات وهياكل الطائرات بسبب نسبة القوة إلى الوزن العالية. غالبًا ما يتم عمل الثقوب على هذه الهياكل لتقليل الوزن وتسهيل الخدمات واعمال الصيانة كما في اضلاع جناح الطائرة. يعاني هذا النوع من الهياكل من ظاهرة الانبعاج بسبب ابعادها ويزداد تعرضها للانبعاج مع وجود الثقوب فيها. بحثت هذه الدراسة تجريبيا وعدديا سلوك الانبعاج لعتبة قناة رقيقة الجدران ذات الشفاه مصنوعة من سبيكة الالمنيوم 6061-O وحاوية على ثقوب ومعرضة الى حمل الانضغاط. تم استخدام طريقة العناصر المحددة اللاخطية في التحليل للحصول على احمال الانبعاج للعتبات. تم اجراء الاختبارات العملية لغرض التحقق من نتائج طريقة العناصر المحددة. تم اختيار ثلاث متغيرات لدراسة تأثيرها على مقاومة الانبعاج للعتبات وهي شكل الثقوب, نسبة الفتح ونسبة التباعد. تم الحصول على نتائج العناصر المحددة باستخدام طريقة تاكوجي لتحديد افضل تركيب من المتغيرات الثلاث للحصول على افضل حمل انبعاج حرج. تم تحديد تأثير كل عامل على حمل الانبعاج الحرج باستخدام طريقة تحليل التباين. اظهرت النتائج ان افضل تركيب من المتغيرات التلاث للحصول على اعلى مقاومة انبعاج هي عندما يكون شكل الثقب سداسي, ونسبة الفتح 1.7 ونسبة التباعد 1.3 كما اظهرت النتائج ان نسبة الفتح هي الاكثر تأثيرا على ظاهرة الانبعاج.

الكلمات الرئيسية: هياكل رقيقة الجدران , الانبعاج, طريقة العناصر المحددة اللاخطية, ثقوب, طريقة تاكوجي

1. INTRODUCTION

Aluminum alloy members are increasingly used in structural applications, especially in bridges and space structures because of their high strength-to-weight ratio, attractive appearance and the perfect corrosion resistance. Furthermore aluminum alloy members are ease of transportation, extrusion and assembly. Recently, these members are often perforated for reducing weight and to facilitate the building services and inspection. These perforations cause a redistribution of stresses in the member that may change the ultimate strength of the structural member and the elastic stiffness. The buckling behavior of structural members with perforations is significantly influenced by the size, location, shape and number of perforations.

There is a lot of investigations have been studied on the design and behavior of aluminum alloy members. **(Hopperstad, Langseth and Tryland, 1999)** investigated experimentally the overall stability of aluminum alloy members of 6082-T4 and 6082-T6 under compression loading with ten different cross-sections. The results were compared with the design strength. **(Mazzolani et al., 2000)** studied the behavior of 6060, 6061 and 6082 aluminum alloy members experimentally with square (SHS) and rectangular (RHS) hollow sections under uniform axial compression load. They established a new classification criterion for sections of aluminum alloy. **(Zhu and Young, 2006)**, **(Zhu and Ã, 2006a)**, and**(Zhu and Ã, 2006b)** investigated buckling behavior of 6063-T5 and 6061-T6 aluminum alloy columns SHS and RHS with five series of specimens in fixed-ended under compression load. Using direct strength method, the design formulae for aluminum alloy

columns were proposed by carrying out numerical investigation and parametric study. **(Yuan, Yuanqing and Bu, 2015)** conducted an experimental tests on 6061-T6 and 6063-T5 aluminum alloy I-section stub columns subjected to compression loading in fixed-ended supports. Local buckling and post buckling behaviors were studied. **(Liu et al., 2015)** studied experimentally the locally buckling failure of 6063-T5 aluminum alloy members with four stiffened closed sections subjected to compressive force. **(Zhao, Zhai and Sun, 2016)** investigated experimentally the buckling behavior of 6068-T6 aluminum alloy extruded columns with L-type and box-type sections under eccentric compression load.

On the other hand, the structural members with perforations have been widely studied on cold-formed steel members. **(Moen and Schafer, 2008)** and **(Moen et al., 2011)** investigated buckling failure of stub and intermediate cold-formed steel columns under compression load with and without slotted web holes. **(Kulatunga and Macdonald, 2013)** studied about the effect of perforation position on the capacity of cold-formed steel lipped channel sections under compression loading by using finite element analysis. In addition, **(Kulatunga et al., 2014)** presented experimentally and numerically the effect of various shapes of perforations on buckling behavior of cold-formed members with lipped channel cross-section.

There are a little investigations being carried out on the aluminum alloy members with perforations. **(Zhou and Young, 2010)** investigated the buckling behavior of 6061-T6 aluminum alloy square hollow sections (SHS) with a circular hole under web crippling. They presented 84 test results and 132 numerical results. **(Feng, Young and Asce, 2015)** studied the failure of SHS stub columns with circular holes under compression load and made a comparison between the test results and design strength using the current design rules for steel structural member with perforations. **(Feng et al., 2018)** tested a total of 64 specimens of 6061-T6 and 6063-T5 aluminum alloy perforated SHS and RHS under axial compression loading and results were compared with Design strength method.

Taguchi is one of the optimization methods that use an orthogonal array, signal-to-noise (S/N) ratio and analyses of variance (ANOVA) to find the best set of parameters and the most influential on buckling strength. Cost and time required to carry out the experiments can be reduced by using Taguchi **(Khamlichi et al., 2010)**, **(Khamlichi and Limam, 2012)**, **(Azadi and Rostamiyan, 2015)**, **(Lin and Lee, 2015)**, **(Soufain et al., 2017)** and **(H.M.AL-khafaji, 2017)**.

In this work, an experimental and numerical study was presented to investigate the buckling behavior of aluminum alloy 6061-O perforated thin-walled lipped channel beam subjected to compression load. Three factors namely; shape of holes, opening ratio D/D_o and spacing ratio S/D_o were chosen to study their influence on buckling strength of beam. Taguchi method was applied to identify the optimum set of parameters that afford the best strength of buckling. Furthermore, the analysis of variance technique (ANOVA) was employed to determine the most effective parameter on the ultimate load.

2. TAGUCHI

Taguchi method is a useful technique and is known as "orthogonal array" for design of experiments. It is the most effective in comparing with the other methods, because it provides an effective and simple way for optimizing and producing high quality products with low cost of manufacturing. This method needs a few numbers of experiments, and so it makes the design of experiments too easy.

This method employs a statistical measurement named as the ratio of the mean (called signal) to the standard deviation (called noise) (S/N), which represents a logarithmic function of wanted

output. There are three standard types of S/N ratio; higher the better,(HB), lower the better,(LB) and Nominal the best,(NB). In this study, the higher buckling strength is required, therefore, the higher the better formula is used and it can be obtained from Eq.(1) below :

$$S/N = -10\ log\ (\frac{1}{n}\sum_{i=1}^{n}\frac{1}{y_i^2}) \quad (1)$$

Where, y_i is the read data and n is the number of observations. This study aim to specify the most effective factors to achieve the higher enhancement of buckling strength of the thin-walled member also to detect the optimum set of factors in a limited number of experiments with using Taguchi method.

3. ANALYSIS OF VARIANCE (ANOVA)

Analysis of variance (ANOVA) is a powerful statistical technique, which specifies the important parameters and demonstrates the percentage contribution of each parameter. In this research, the ratio (S/N) was used for making the decision. The technique of ANOVA is based on the total sum of squared deviations (SST) which is equal to **(Kabe and Gupta, 2010)**:

$$SS_T = \sum_{i=1}^{n}(n_i - n_m)^2 \quad (2)$$

The percentage contribution P could be calculated as:

$$P = \frac{SS_d}{SS_T} \quad (3)$$

$$d.o.f\ of\ any\ parameter\ (factor) = k - 1 \quad (4)$$

$$Total\ d.o.f = n - 1 \quad (5)$$

$$d.o.f\ of\ error = total\ d.o.f - \sum d.o.f\ of\ parameters \quad (6)$$

$$V = \frac{SS_d}{d.o.f} \quad (7)$$

$$F = \frac{V}{V_E} \quad (8)$$

Where:
n : The number of observation (trails) in the orthogonal array.
n_i: mean S/N ratio for the ith observation.
n_m : mean of all parameters.
SS_d: A sum of the squared deviations.
K : The number of levels for each parameter.
P : Contribution's percentage.
V: Parameter's (factor) variance.
V_E: Error's variance.
$d.o.f$: A degree of freedom.
F: F - test, which is an indicator of the quality characteristic of the process.

4. EXPERIMENTAL PROGRAM

4.1 Material properties

Aluminum alloy 6061-O sheets with 1.6 mm thickness were used to manufacture the specimens. Tensile tests were conducted to validate the mechanical properties of sheets. Tests were done on the tensile specimens according to ASTM specifications B557M-02a **(International, 2003)** and test results were indicated in **Table 1.**

Table 1. The mechanical properties of aluminum alloy 6061-O.

Aluminum 6061-O	Young modulus E(Gpa)	Poisson's ratio υ	Yield stress (Mpa)σ_y	Ultimate stress (Mpa)σ_u
Experimental measured (average of three specimens)	68.9	0.33	50	109

4.2 Specimen geometry

4.2.1 Design of cross-section

The cross-section dimensions designed according to the following design constraints of Eurocode (EN-1993-1-3) **(CEN, 2006)** and it shown in **Fig. 1**. The beam length is intermediate and it is (500mm) for all specimens.

$$b/t \leq 60, a/t \leq 50, D/t \leq 500 \quad (9)$$

$$0.2 \leq a/b \leq 0.6 \quad (10)$$

$$a \leq 25 \quad (11)$$

Where D is the cross-section width, b is the flange width, a is the lip width and t is the thickness. Eq. (9) refers to the design limits of width-to-thickness ratios set by the Eurocode (EN-1993-1-3) for the lipped channel cross-sections, whereas Eqs. (10) and (11) provide sufficient stiffness and to prevent the primary buckling of the lip itself according to Clause 5.2.2 of the Eurocode.

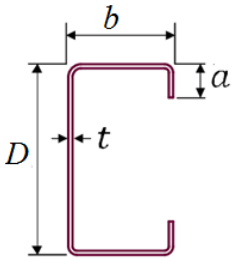

Cross-section	
D (mm)	100
b (mm)	38
a (mm)	12
t (mm)	1.6

Figure 1. Specimen cross-section dimensions.

4.2.2 Design of holes

In this work, three shapes of holes designed to be made in the web as shown in **Fig. 2** with dimensions according to the limits of applicability of web holes of cellular beam in Eurocode (BS-5950) by Eqs. (12) and (13). The geometry of web holes must be within the given ranges of Eurocode in order to prevent any unwanted failures like cracks between holes, and to achieve a maximum possible reduction in weight.

$$1.25 < D/D_O < 1.75 \quad (12)$$

$$1.08 < S/D_O < 1.5 \quad (13)$$

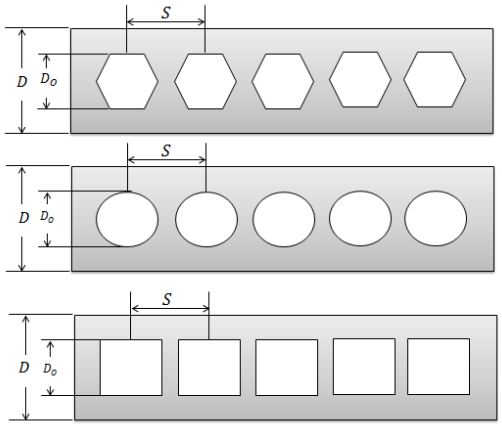

Figure 2. Shapes of holes and dimensions.

Table 2. shows the chosen parameters in three levels for analysis, namely:

- Shape of holes
- Opening ratio (D/D_o)
- Spacing ratio (S/D_o)

Table 2. Parameters and levels.

symbols	parameter	Levels		
		Level 1	Level 2	Level 3
A	Shape of holes	Hexagonal	Circular	Square
B	D/D_o	1.7	1.6	1.5
C	S/D_o	1.5	1.4	1.3

4.3 Specimens preparing

A total of four specimens were tested in this work to verify the numerical solution. One of them without holes as a reference beam and the other three specimens had five holes with shapes of (hexagonal, circular and square) as shown in **Fig. 3**. The cross-section of lipped beams was made by flexing the Aluminum alloy 6061-O sheet by using a hydraulic bending press machine. The axes were programed by a control system to achieve accurate positions of the inverter for giving accurate dimensions of cross-section. A water jet process was used to make holes on the web of

the beam to get a good surface finishing and to minimize any residual stresses at the area of the holes.

Figure 3. Test specimens.

4.4 Buckling test

The WDW-200E computer Controlled Electronic Universal Testing Machine was used for testing the specimens for buckling failure under compression loading. Four specimens of thin-walled lipped channels were tested in fixed-fixed end condition by applying an axial compressive force at the upper face of the specimen until failure. Two of identical fixing attachments were designed and manufactured to fix the channel on the machine to prevent any displacement or rotation of cross-section. Two solid cubes of Teflon with dimensions of (96.5*34.5*20) mm^3 put between the flanges at beam ends in order to prevent any relative motion or distortion of cross-section parts at the beam ends due to loading**. Fig.4** shows the ends fixture with the inside and outside attachments. The load is gradually applied at rate of 0.3 mm/min by the controlling computer. The load-displacement curve was obtained and the results were recorded. **Fig. 5** shows the buckling test under compression loading.

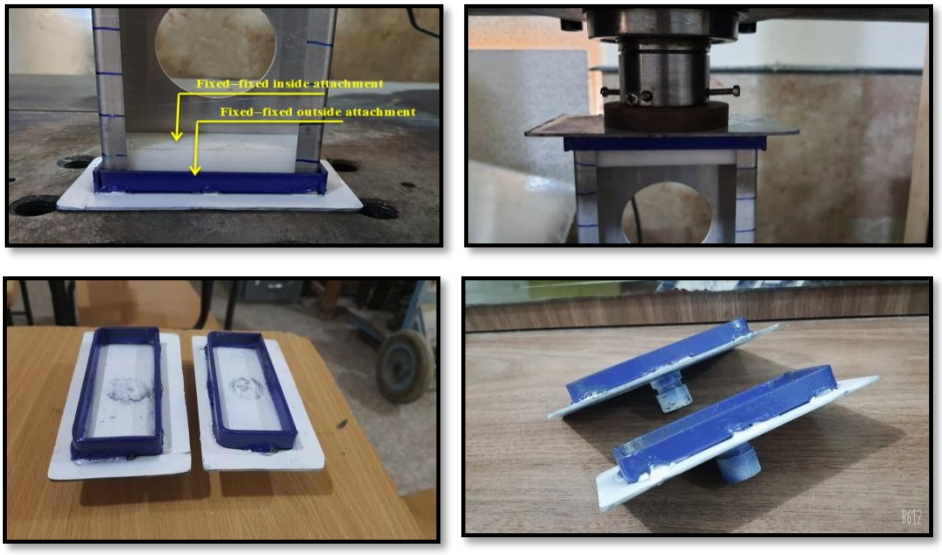

Figure 4. The ends fixture for fixed-fixed end condition of the compression test.

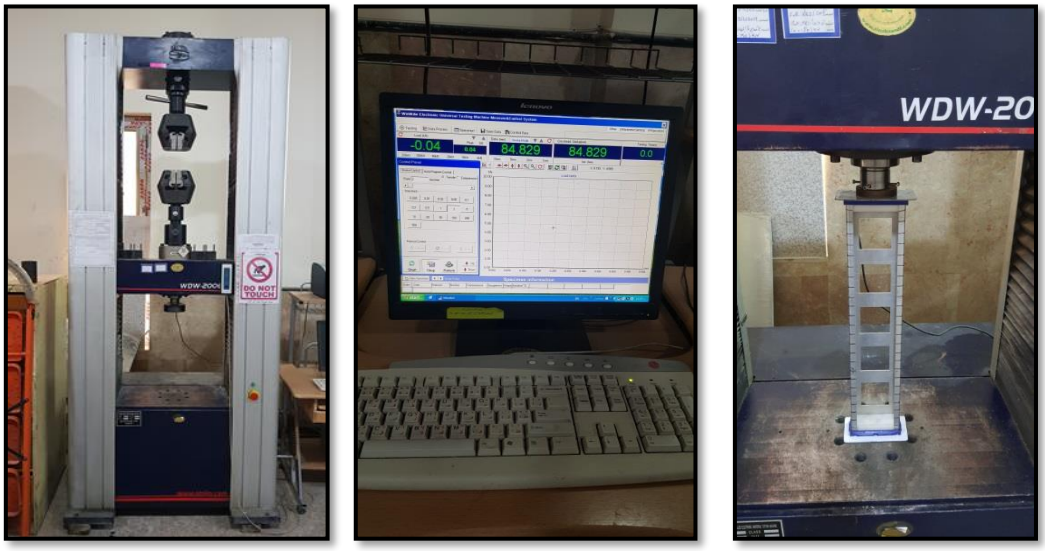

Figure 5. Buckling test under compression loading.

5. FINITE ELEMENT ANALYSIS

5.1 Modeling

The perforated beams are modeled and analyzed in ANSYS 15 software by finite element analysis using SHELL181. It is defined by four nodes having six degrees of freedom at each node, translations in the x, y, and z directions, and rotations about the x, y, and z-axes. SHELL181 is well-suited for linear, large rotation, and/or large strain nonlinear applications **(Madenci and Guven, 2006)** as shown in **Fig. 6**. The mesh convergence was established by increased the mesh density in each part of the model. It was observed that there were no considerable changes in load response between 10 mm and 4 mm element size but the processing time was considerable and any increment in mesh density is unnecessary as shown in **Fig. 7**. Therefore, Element size of 10 mm was used in subsequent analysis.

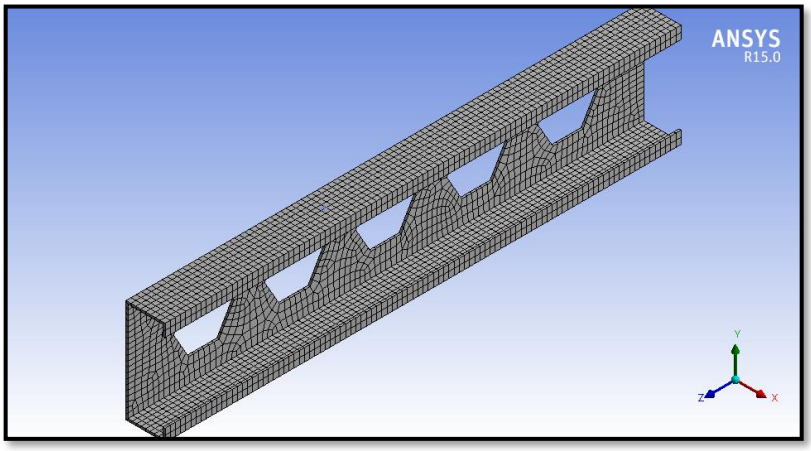

Figure 6. Models of the beam.

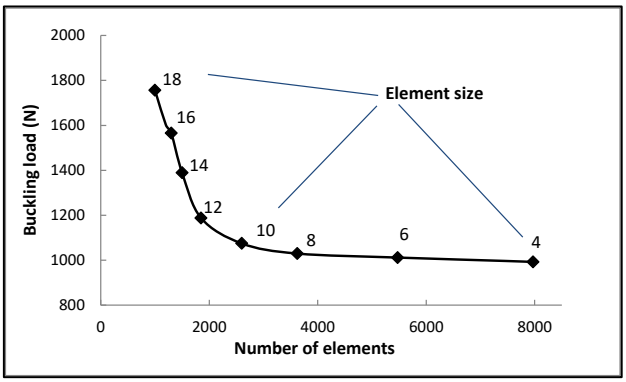

Figure 7. Graph of buckling load against number of elements (mesh density).

5.2 Boundary conditions and loads

Boundary conditions are needed to constrain the model to get a unique solution. To achieve this, all translations (UX, UY, and UZ) and rotations (ROTX, ROTY and ROTZ) for all points at the bottom end are restrained in order to obtain a fixed support. The rotations about the three directions and the translation along the axial direction for the points at the top end are also restrained. The force F is applied on the upper face of the model as shown in **Fig. 8**. The first mode shape from the eigen buckling analysis was used to prepare the initial deformed model which will be used later in the nonlinear buckling analysis as a beam with initial imperfection. The main purpose of using nonlinear analysis is to obtain the ultimate capacity of the beam.

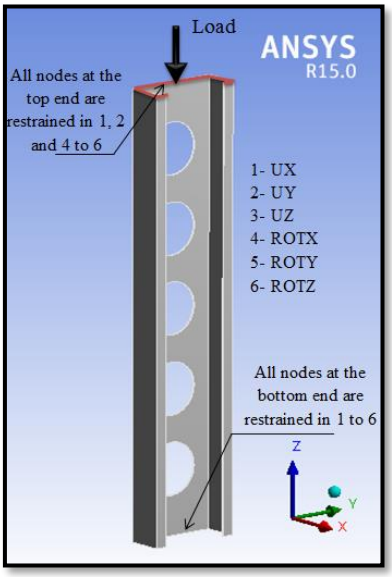

Figure 8. Load and boundary conditions on the beam.

6. RESULTS

6.1 Test Results

The test results showed that the buckling mode of failure of the lipped channels under compression loading is an interaction of local and distortional buckling as shown in **Fig. 9**. As it is clear from **Fig.9**, the flanges were distorted in a half-wave for all specimens in the longitudinal axes. It may happen due to the high compression stresses generated on the flanges plane during loading process,

making the stiffener has no enough stiffness to prevent the flange from rotating, that lead the flanges to rotate at the flange/web junction, outward or inward depending on the nature of the load, supporting system or imperfections. Many buckles can be seen clearly along the web of the reference channel (i.e. the channel without holes) and near the edges of the holes of the perforated channels. Local buckling often occurs at a lower load than the distortional buckling and both are lower than the ultimate load. During the test, the local buckles began to appear approximately at 40% of the ultimate load and the distortional buckling was occur approximately at 80% of the ultimate load. The load-displacement curves that obtained from the experimental tests were shown in **Fig. 10** and the results of ultimate load were indicated in **Table 3**. It was clear that the presence of perforations causing a decrease in the ultimate loads of the channels with a percentage reduction of 9.14% for the hexagonal hole shape, 13.85% for the circular hole shape and a maximum percentage reduction of 15.24% for the square hole shape. Test results were used to validate the FEM results.

Figure 9. Specimens after buckling test under compression loading.

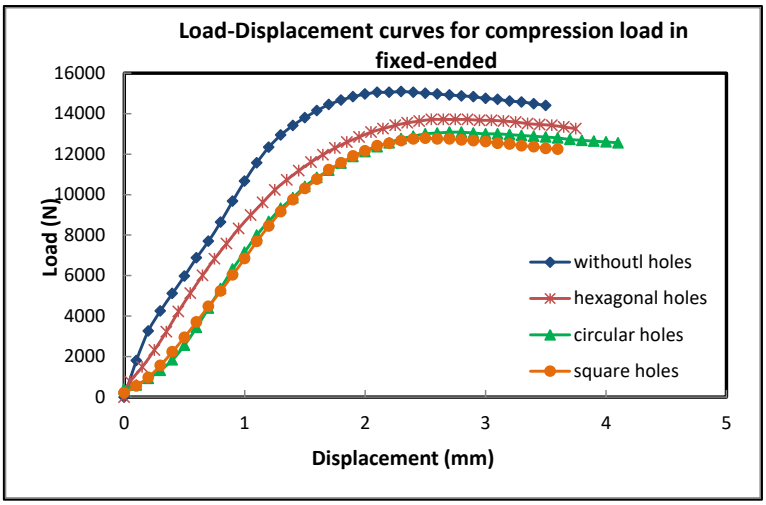

Figure 10. The experimental load-displacement curves for beams under compression load.

Table 3. Specimens hole dimensions and experimental results.

Shape of holes	D/D_O	S/D_O	P exp.(N)
Without holes (Ref.)	-----	-----	15090
Hexagonal	1.7	1.5	13710
Circular	1.7	1.5	13000
Square	1.7	1.5	12790

6.2 Validation of FEM Results

The ANSYS version (15) analysis gave a good agreement with the experimental results and a comparison of load-displacement curves between the experimental tests and the numerical simulations were done and indicated in **Fig. 11**. In the nonlinear solution, the load was applied gradually by load steps and sub-steps and the ultimate load was reading at where the non-converged solution occurs. It was clear from the simulation results that ultimate strength of the thin-walled beam decreases with the presence of holes on the web when subjected to compression loading with a minimum percentage reduction of 9.99% for the hexagonal hole shape and a maximum of 15.86% for the square hole shapes as shown in **Table 4** and **Fig. 12**. The buckling failure mode was in agreement with the actual test failure and the half-waves of the distortional buckling failure for all types of holes were evident in **Fig. 13**.

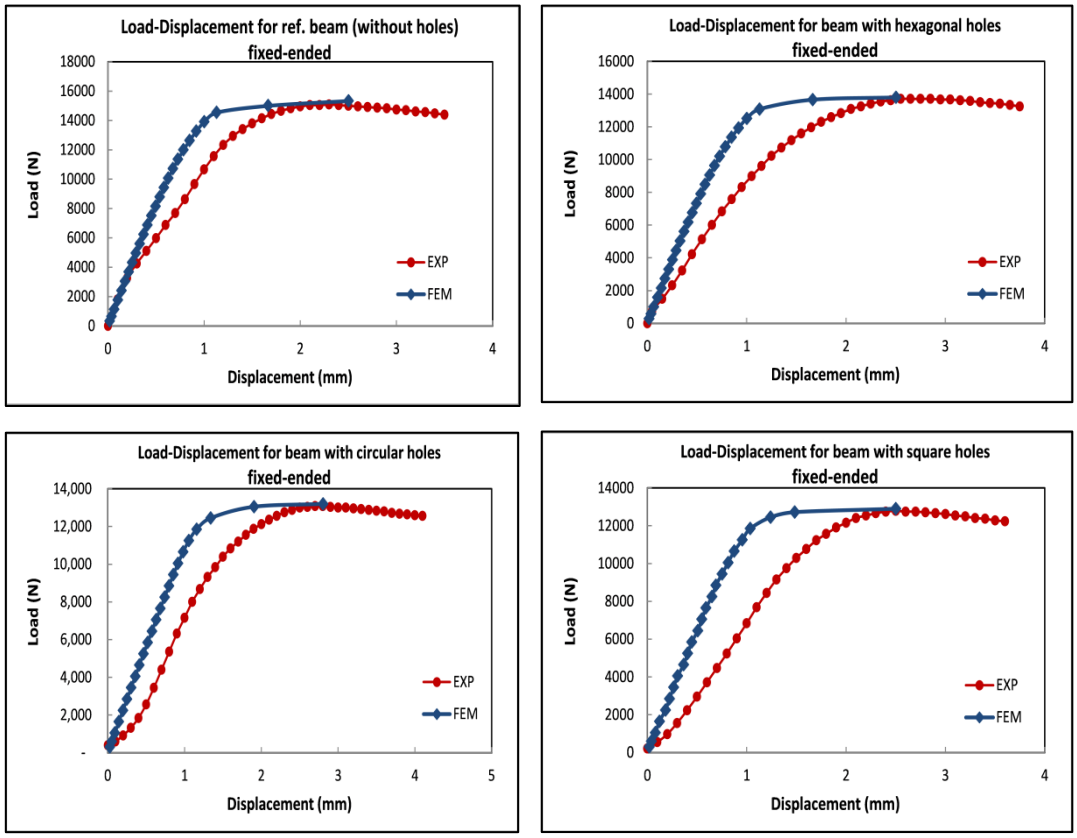

Figure 11. Comparison of load-displacement curves between experimental and numerical results.

Table 4. Comparison of ultimate loads between experimental and numerical results.

Shape of holes	Opening ratio (D/D_O)	Spacing ratio (S/D_O)	(N)$P_{EXP.}$	P_{FEM} (N)	/ $P_{FEM}P_{EXP}$
Without holes	----	----	15090	15332	0.98
Hexagonal	1.7	1.5	13710	13800	0.99
Circular	1.7	1.5	13000	13200	0.98
Square	1.7	1.5	12790	12900	0.99

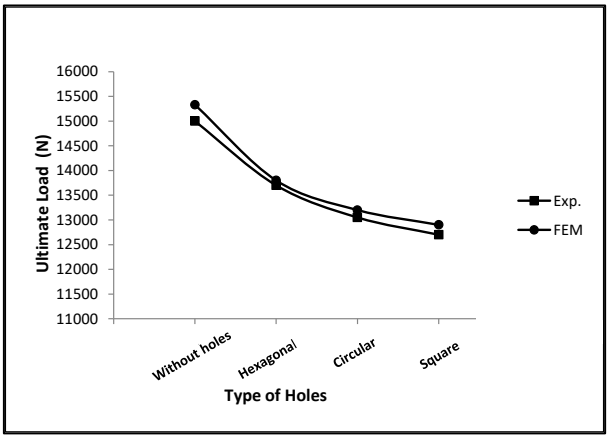

Figure 12. Comparison of ultimate loads between numerical and experimental results.

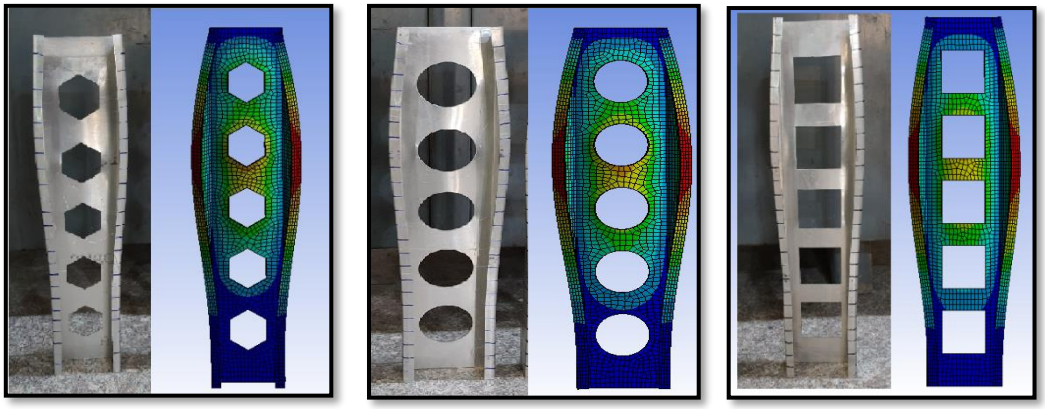

Figure 13. Comparison of failure mode of the perforated lipped channels between numerical and experimental results.

6.3 Finite element Results

Nonlinear finite element analyses were performed to calculate the ultimate load. In this study, the strength-to-weight ratio was used for the optimization process due to its importance in the lightweight structures especially with exist of perforators. According to three parameters and three levels, an orthogonal array L27 was established, as presented in **Table 5**. So, the twenty-seven value of ultimate load was got from different combinations of parameters' levels.

Table 5. Orthogonal array for levels combinations and corresponding ultimate loads.

N0. of test	Shape of holes	Opening ratio (D/D_O)	Spacing ratio (S/D_O)	Ultimate load (N)	Weight (N)	$\frac{\text{strength}}{\text{wieght}}$
1	Hexagonal	1.7	1.5	13800	3.6262	3805.64
2	Circular	1.7	1.5	13200	3.5265	3743.09
3	Square	1.7	1.5	12900	3.3691	3828.92
4	Hexagonal	1.6	1.5	13321	3.5647	3736.92
5	Circular	1.6	1.5	12768	3.4551	3695.41
6	Square	1.6	1.5	12272	3.2746	3747.63
7	Hexagonal	1.5	1.5	11332	3.4906	3246.43
8	Circular	1.5	1.5	10471	3.3626	3113.96
9	Square	1.5	1.5	9872.4	3.1605	3123.68
10	Hexagonal	1.7	1.4	14214	3.6262	3919.81
11	Circular	1.7	1.4	13324	3.5265	3778.25
12	Square	1.7	1.4	13052	3.3691	3874.03
13	Hexagonal	1.6	1.4	13651	3.5647	3829.49
14	Circular	1.6	1.4	12872	3.4551	3725.51
15	Square	1.6	1.4	12452	3.2746	3802.60
16	Hexagonal	1.5	1.4	13052	3.4906	3739.19
17	Circular	1.5	1.4	12002	3.3626	3569.26
18	Square	1.5	1.4	11618	3.1605	3676.00
19	Hexagonal	1.7	1.3	14300	3.6262	3943.52
20	Circular	1.7	1.3	13450	3.5265	3813.98
21	Square	1.7	1.3	13200	3.3691	3917.96
22	Hexagonal	1.6	1.3	13850	3.5647	3885.32
23	Circular	1.6	1.3	13000	3.4551	3762.55
24	Square	1.6	1.3	12661	3.2746	3866.43
25	Hexagonal	1.5	1.3	13202	3.4906	3782.16
26	Circular	1.5	1.3	12272	3.3626	3649.56
27	Square	1.5	1.3	11792	3.1605	3731.06

6.4 Taguchi and ANOVA results

The orthogonal array and values of S/N was shown in **Table 6** and Results of mean based on S/N were presented in **Table 7** and **Fig. 14:**

Table 6. Orthogonal array and S/N.

N0. of test	Shape of holes -A-	(D/D_O) -B-	(S/D_O) -C-	$\frac{\text{strength}}{\text{wieght}}$	S/N
1	Hexagonal	1.7	1.5	3805.64	71.609
2	Circular	1.7	1.5	3743.09	71.465
3	Square	1.7	1.5	3828.92	71.662
4	Hexagonal	1.6	1.5	3736.92	71.450

5	Circular	1.6	1.5	3695.41	71.353
6	Square	1.6	1.5	3747.63	71.475
7	Hexagonal	1.5	1.5	3246.43	70.228
8	Circular	1.5	1.5	3113.96	69.866
9	Square	1.5	1.5	3123.68	69.893
10	Hexagonal	1.7	1.4	3919.81	71.865
11	Circular	1.7	1.4	3778.25	71.546
12	Square	1.7	1.4	3874.03	71.763
13	Hexagonal	1.6	1.4	3829.49	71.663
14	Circular	1.6	1.4	3725.51	71.424
15	Square	1.6	1.4	3802.60	71.602
16	Hexagonal	1.5	1.4	3739.19	71.456
17	Circular	1.5	1.4	3569.26	71.052
18	Square	1.5	1.4	3676.00	71.308
19	Hexagonal	1.7	1.3	3943.52	71.918
20	Circular	1.7	1.3	3813.98	71.628
21	Square	1.7	1.3	3917.96	71.861
22	Hexagonal	1.6	1.3	3885.32	71.789
23	Circular	1.6	1.3	3762.55	71.510
24	Square	1.6	1.3	3866.43	71.746
25	Hexagonal	1.5	1.3	3782.16	71.555
26	Circular	1.5	1.3	3649.56	71.245
27	Square	1.5	1.3	3731.06	71.437

From **Table 7** and **Fig. 14** it was seen that the optimum set of levels is (A1 B1 C3) which gives the best ultimate buckling strength and best strength to weight ratio. The combination of parameters is the hexagonal hole shape, $D/D_o = 1.7$ and $S/D_o = 1.3$. Delta column refer to the deference between the maximum and minimum level value. It shows that the opening ratio D/D_o has more effect on buckling strength than the other parameters. The rank column indicates the order of parameters from the highest to the lowest influential on buckling strength depending on Delta values. **Fig. 15** shows the numerical load-displacement curve for the condition (A1 B1 C3).

Table 7. The analysis of mean results based on S/N.

symbols	parameters	Level 1	Level 2	Level 3	Delta	Rank
A	Shape of holes	71.504	71.232	71.416	0.272	3
B	D/D_O	71.702	71.557	70.893	0.809	1
C	S/D_O	71.000	71.520	71.632	0.632	2

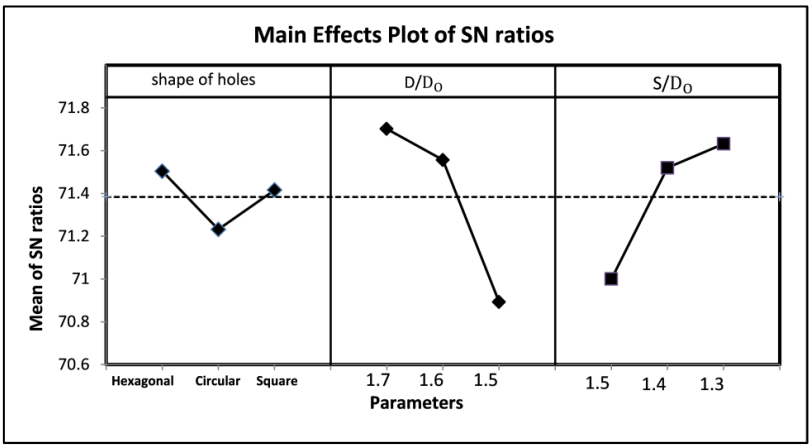

Figure 14. The parameters – S/N curves.

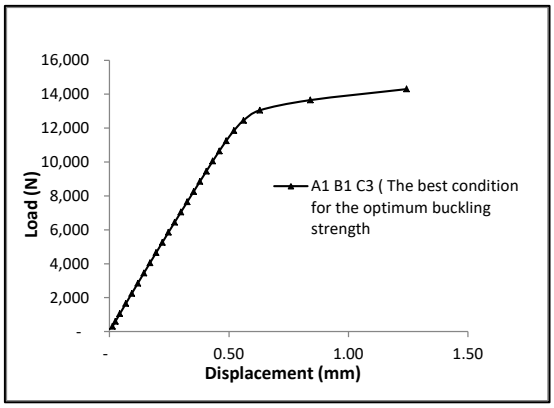

Figure 15. The load-displacement curve of the A1 B1 C3 condition (the optimum set).

Table 8 shows the results of ANOVA. These results represent the importance and contribution of parameters as a percentage. The opening ratio has the highest contribution (44.05%) and the lowest effect is the shape of holes (4.56%).

Table 8. Results of (ANOVA).

Source		Sum sq.	d.o.f.	Mean sq.	F	P %
A	Shape	0.346	2	0.173	1.86	4.56
B	D/Do	3.345	2	1.673	17.99	44.05
C	S/Do	2.045	2	1.023	11	26.93
Error		1.856	20	0.093		
Total		7.593	26			

7. CONCLUSION

This research investigated the buckling behavior of perforated aluminum alloy 6061-O thin-walled lipped channel beam under compression loading and studied the effect of three factors namely shape of holes, opening ratio D/D_o and the spacing ratio of S/D_o on ultimate strength and the strength-to-weight ratio of the perforated beam. This study also aims to obtain the best set of factors which gives the optimum ultimate buckling strength and the most influential factor on the ultimate load. A finite element method was implemented to investigate the buckling behavior of the beam under a compression load. The finite element models were validated by experimental experiences by using four specimens. Taguchi and ANOVA methods were implemented to confirm the effect of parameters and their combinations. From the results obtained, the following conclusions can be obtained:

1- In the experimental tests, it was found that the hexagonal hole shape causes a less reduction in ultimate strength compared with the other hole shapes (9.14%), while the square hole shape had a larger reduction (15.24%).
2- The combination of parameters that gives the best ultimate strength is the hexagonal hole shape, $D/D_o = 1.7$ and $S/D_o = 1.3$
3- The opening ratio has the highest contribution (44.05%) on the buckling strength and the lowest influential is the shape of holes (4.56%).

NOMENCLATURE

a = lip width, mm
b = width of the flange, mm
D = width of the web, mm
D_O = diameter of the hole, mm
E = Young modulus, Gpa
K = number of levels for each parameter
$n =$ number of observation (trails) in the orthogonal array.
n_i = mean S/N ratio for the ith observation.
n_m = mean of all parameters.
P =contribution's percentage.
P_{EXP}= experimental ultimate buckling load, N
P_{FEM} = numerical ultimate buckling load, N
SS_d = sum of the squared deviations.
S = space between two holes centers, mm
t = thickness of the beam, mm
V = parameter's variance.
V_E = error's variance.
y_i= the read data for the higher the better formula of Taguchi
υ = poisson's ratio
σ_y = yield stress, Mpa
σ_u = ultimate stress, Mpa

REFERENCES

- Azadi, R. and Rostamiyan, Y. (2015) 'Experimental and analytical study of buckling strength of new quaternary hybrid nanocomposite using Taguchi method for optimization', *Construction and Building Materials*. Elsevier Ltd, 88, pp. 212–224. doi: 10.1016/j.conbuildmat.2015.04.018.
- CEN (2006) 'EN1993-1-3 Eurocode 3: Design of steel structures - part 1-3: supplementary rules for cold-formed members and sheeting', in *European Committee for Standardization, Brussels*.
- Feng, R. *et al.* (2018) 'Tests of perforated aluminium alloy SHSs and RHSs under axial compression', *Thin-Walled Structures*. Elsevier Ltd, 130, pp. 194–212. doi: 10.1016/j.tws.2018.03.017.
- Feng, R., Young, B. and Asce, M. (2015) 'Experimental Investigation of Aluminum Alloy Stub Columns with Circular Openings', *Journal of Structural Engineering*, 141(11), pp. 1–10. doi: 10.1061/(ASCE)ST.1943-541X.0001265.
- Hopperstad, O. S., Langseth, M. and Tryland, T. (1999) 'Ultimate strength of aluminium alloy outstands in compression : experiments and simplified analysis', *Thin Walled Structures*, 34(0263), pp. 279–294.
- International, A. (2003) 'B 557 M - 02a: Standard test methods of tension testing wrought and cast aluminum- and magnesium-alloy products [metric]', 03.
- Kabe and Gupta (2010) *Experimental Design; Exercises & Solutions, Antimicrobial Agents and Chemotherapy*. doi: 10.1088/1751-8113/44/8/085201.
- Khamlichi, A. *et al.* (2010) 'Effect of two interacting localized defects on the critical load for thin cylindrical shells under axial compression', *American Journal of Engineering and Applied Sciences*, 3(2), pp. 464–469. doi: 10.3844/ajeassp.2010.464.469.
- Khamlichi, A. and Limam, A. (2012) 'Assessing the effect of two entering triangular initial geometric imperfections on the buckling strength of an axisymmetric shell subjected to uniform axial compression', *Civil-Comp Proceedings*, 99, pp. 1–11. doi: 10.4203/ccp.99.166.
- Kulatunga, M. P. *et al.* (2014) 'Load capacity of cold-formed column members of lipped channel cross-section with perforations subjected to compression loading - Part I: FE simulation and test results', *Thin-Walled Structures*. Elsevier, 80, pp. 1–12. doi: 10.1016/j.tws.2014.02.017.
- Kulatunga, M. P. and Macdonald, M. (2013) 'Investigation of cold-formed steel structural members with perforations of different arrangements subjected to compression loading', *Thin-Walled Structures*. Elsevier, 67, pp. 78–87. doi: 10.1016/j.tws.2013.02.014.
- Lin, J. C. and Lee, K. (2015) 'Optimization of bending process parameters for seamless tubes using Taguchi method and finite element method', *Advances in Materials Science and Engineering*, 2015, pp. 1–8. doi: 10.1155/2015/730640.
- Liu, M. *et al.* (2015) 'Experimental investigation on local buckling behaviors of stiffened closed-section thin-walled aluminum alloy columns under compression', *Thin Walled Structures*. Elsevier, 94, pp. 188–198. doi: 10.1016/j.tws.2015.04.012.
- M.AL-khafaji, H. (2017) 'Best level of parameters for a critical buckling load for circular thin- walled structure subjected to bending', *Al-Khwarizmi Engineering Journal*, 13(4), pp. 12–21. doi: 10.22153/kej.2017.07.003.

- Madenci, E. and Guven, I. (2006) *The finite element method and applications in engineering using ANSYS*. the university of Arizona.
- Mazzolani, F. M. *et al.* (2000) 'Local Buckling of Aluminum Members : Testing and Classification', *Journal of Structural Engineering*, 126, pp. 353–360. doi: 10.1061/(ASCE)0733-9445(2000)126.
- Moen, C. D. *et al.* (2011) 'Direct Strength Method for Design of Cold-Formed Steel Columns with Holes', *Journal of Structural Engineering*, 137, pp. 559–570. doi: 10.1061/(ASCE)ST.1943-541X.0000310.
- Moen, C. D. and Schafer, B. W. (2008) 'Experiments on cold-formed steel columns with holes', *Thin-Walled Structures*, 46(10), pp. 1164–1182. doi: 10.1016/j.tws.2008.01.021.
- Soufain, M. J. *et al.* (2017) 'Analytical investigation for buckling capacity of composite steel tubes under compression – Taguchi ' s approach using Minitab-16', *international journal of innvative research in science engineering and technology*, 6(4), pp. 6645–6655. doi: 10.15680/IJIRSET.2017.0604079.
- Yuan, H., Yuanqing, W. and Bu, Y. (2015) 'Local buckling and postbuckling strength of extruded aluminium alloy stub columns with slender I-sections', *Thin Walled Structures*, 90, pp. 140–149. doi: 10.1016/j.tws.2015.01.013.
- Zhao, Y., Zhai, X. and Sun, L. (2016) 'Test and design method for the buckling behaviors of 6082-T6 aluminum alloy columns with box-type and L-type sections under eccentric compression', *Thin-Walled Structures*. Elsevier, 100, pp. 62–80. doi: 10.1016/j.tws.2015.12.010.
- Zhou, F. and Young, B. (2010) 'Web crippling of aluminium tubes with perforated webs', *Engineering Structures*. Elsevier Ltd, 32(5), pp. 1397–1410. doi: 10.1016/j.engstruct.2010.01.018.
- Zhu, J. and Ã, B. Y. (2006a) 'Aluminum alloy tubular columns — Part I : Finite element modeling and test verification', *Thin Walled Structures*, 44, pp. 961–968. doi: 10.1016/j.tws.2006.08.011.
- Zhu, J. and Ã, B. Y. (2006b) 'Aluminum alloy tubular columns — Part II : Parametric study and design using direct strength method', *Thin-Walled Structures*, 44, pp. 969–985. doi: 10.1016/j.tws.2006.08.012.
- Zhu, J. H. and Young, B. (2006) 'Tests and design of aluminum alloy compression members', *Journal of Structural Engineering*, 132(7), pp. 1096–1107. doi: 10.1061/(ASCE)0733-9445(2006)132:7(1096).